

MECHANISMS OF STRUCTURE FORMATION AND HARDENING IN A DEFORMED HIGH-STRENGTH CAST IRON

Authors: **POKROVSKIY A.I.¹, LASKOVNEV A.P.¹, DUDETSKAYA L.R.¹, KHROL' I.N.¹, KHINA B.B.¹, POKROVSKAYA T.M.²**

Workplace: ¹*Physico-Technical Institute, National Academy of Sciences of Belarus,*
²*Diksan-Auto Co., Ltd.*

Email: **arturu@tut.by**

Abstract:

The anisotropy of structure and properties of high-strength cast iron after hot plastic deformation by extrusion is examined and the basic mechanisms of the effect of deformation on mechanical properties are evaluated. The main factors influencing strengthening are studied: the phase composition of metal matrix, its dispersity and grain morphology, shape and distribution of graphite inclusions. An attempt is made to qualitatively estimate the contribution of structural parameters into overall strain hardening of deformed cast iron and a formula is proposed that connects the compression strength with the characteristics of microstructure.

INTRODUCTION

Cast irons occupy a prominent place among structural materials, and a tendency persists to increase the usage of high-quality grades of cast iron. This is due to better casting and technological properties of cast iron in comparison with steel, a lower melting temperature and better machinability. Being a multicomponent and multiphase system whose ingredients can be purposefully changed, this material permits obtaining a wide variety of microstructures and properties. Cast irons possess certain unique properties. For example, the presence of graphite inclusions provides good antifriction properties, the ability for damping vibrations and resonance oscillations, low notch sensitivity, a lower density as compared with steels and higher thermal conductivity. All of this motivates a wide application of cast irons for critical parts such as cylinder blocks, crankshafts and camshafts, brake drums, clutch disks, piston rings, etc.

The mechanical properties of cast irons can be improved using alloying, inoculation and heat treatment. In particular, isothermal quenching permits attaining the strength of 1000-1200 MPa combined with the elongation to failure of about 2-10%. A further improvement of properties is hampered by the inherent drawbacks of traditional casting technologies, e.g., low and non-uniform properties of castings, low utilization ratio, and some other factors.

Current situation in this area necessitates finding unconventional means for shaping and microstructure controlling of cast-iron parts. World experience has convincingly demonstrated that casting is not the only way of shaping cast-iron articles; in certain temperature and stress conditions this material can be plastically deformed [1-3]. Along with shaping, deformation permits substantially improving the mechanical properties of cast irons.

Of particular interest is the reported increase in the mechanical and service properties of deformed cast iron by the factor of 1.5-2.5 as compared with the as-cast state [4, 5]. It has been established that for attaining maximal strength characteristics in a deformed state, most promising are the irons with compact-shape graphite inclusions, viz. high-strength and malleable cast irons [6]. In their mechanical properties after deformation, such cast irons are competitive with alloy steel and can even exceed the latter in service performance. A gain in

the obtained properties overrides the difficulties associated with plastic working of cast irons and substantially extends their applicability for critical machine parts [7, 8].

However, the dependence of the mechanical properties and service performance of deformed cast iron on the temperature and stress conditions of plastic working are insufficiently studied; the same refers to the structural anisotropy of the material. Thus, the potentiality of deformed cast iron has not been revealed in full.

In this connection, the objective of this research is to investigate the strengthening and structure modification of cast iron due to deformation and estimate the effect of different processing and structural factors on mechanical properties.

Experimental Procedure

The high-strength cast iron studied in this work had the following composition (wt.%): 3.2-3.6% C, 1.7-2.1% Si, 0.5-0.7% Mn, 0.4-0.6% Ni, 0.04-0.06% Mg, <0.08% P and <0.01% S. The microstructure of material in the initial (as-cast) state is shown in Fig. 1.

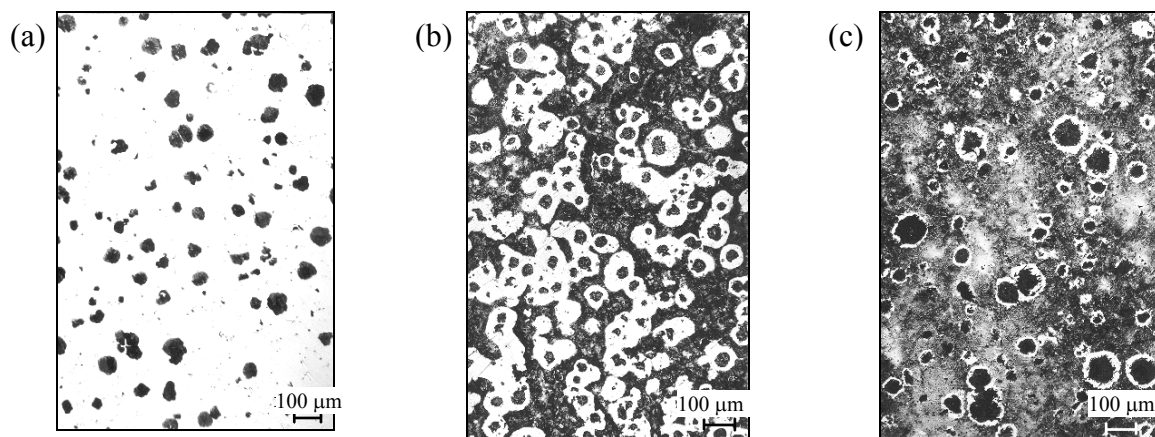


Fig. 1 Microstructure of high-strength cast iron in the initial (non-deformed) state, $\times 100$: (a) as-cast, unetched, (b) as-cast, etched, and (c) cast material after normalizing at 950 °C, etched.

Graphite inclusions have a regular spherical shape (Fig. 1, a) and their diameter doesn't exceed 25-45 μm , the volume fraction of graphite is about 6-10%. The metal matrix consists of pearlite having a high degree of dispersity and ferrite whose content is below 30% (Fig. 1, b). After normalizing at the temperature corresponding to the deformation temperature (950 °C) the fraction of ferrite in the microstructure decreases to 5-10% and it is mainly located as ferrite fringes around graphite inclusions (Fig. 1, c).

Billets of different diameters were subjected to hot extrusion (in the austenitic state) with the reduction ratio of 20-80% through a die to produce rods. Schematic of the extrusion process is shown in Fig. 2.

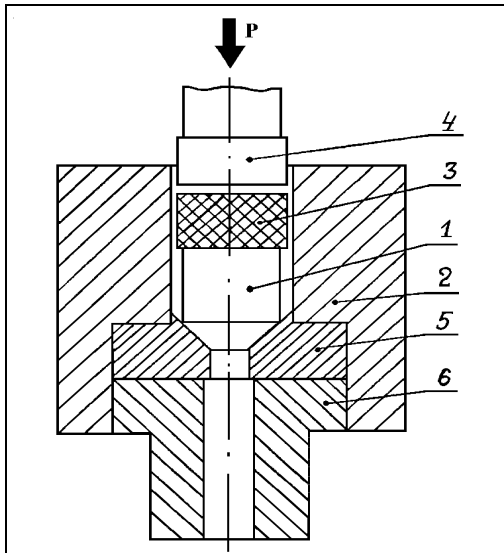


Fig. 2 A schematic chart of plastic deformation of billets by hot extrusion: cast iron billet (1), frame (2), high-strength graphite insert (3), punch (4), extrusion die (5), and guide bush (6)

The shape of the obtained rods is shown in Fig. 3. It is seen that the side surface of an extruded rod contains a large number of cavities having an elongated shape, which appear on the sites of graphite inclusions (Fig. 3, c). This surface morphology with pits, which act as “pockets” for a lubricant, is advantageous for materials used in friction pairs.

The longitudinal and cross-cut specimens for mechanical testing, which were cut out from the extruded rods, are presented schematically in Fig. 4. The shape of elongated graphite inclusions inside the specimens and the fracture plane of samples used in impact-strength tests (Fig. 4, c and f) are shown; besides, shown is the wearing surface of samples used in wear tests (Fig. 4, d and g).

Results and Discussion

After hot extrusion, major changes in the shape of graphite inclusions occur in the longitudinal direction (Fig. 5): they stretch along the direction of metal flow thus acquiring a specific deformation texture. At relatively small strains, $\epsilon \leq 20\%$, the inclusions still retain a round shape while at $\epsilon = 60\%$ they become elongated with pointed ends. With increasing strain to $\epsilon = 80\%$ the graphite inclusions convert into spindles, needles and filaments.

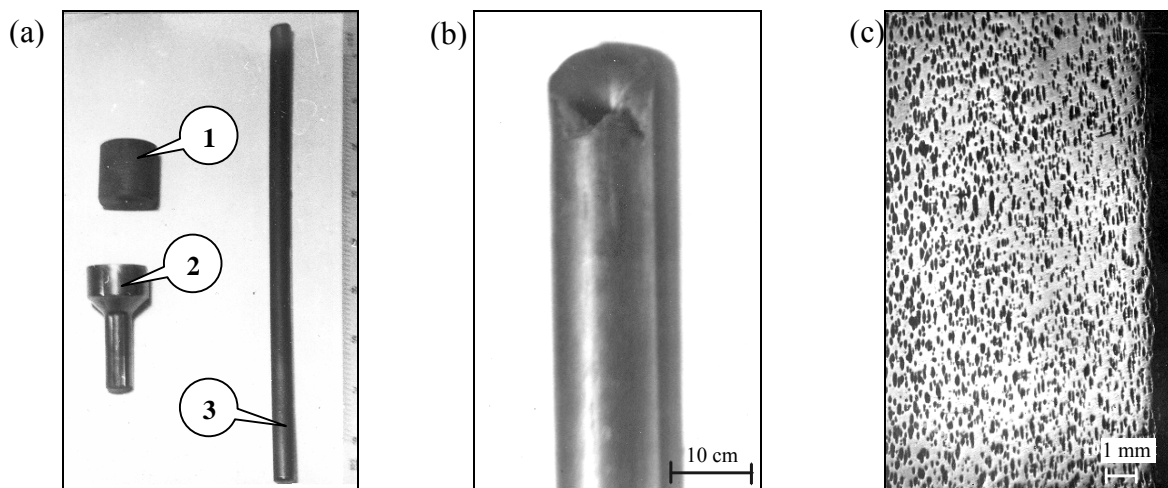


Fig. 3 Hot extrusion of high-strength cast iron: (a) stages of extrusion: initial billet (1), an extruded rod with a butt-end (2) and a rod extruded with the reduction ratio of 80% (3); (b) image of the obtained rod, and (c) surface of a rod produced by hot extrusion with the reduction ratio of 60% ($\times 10$).

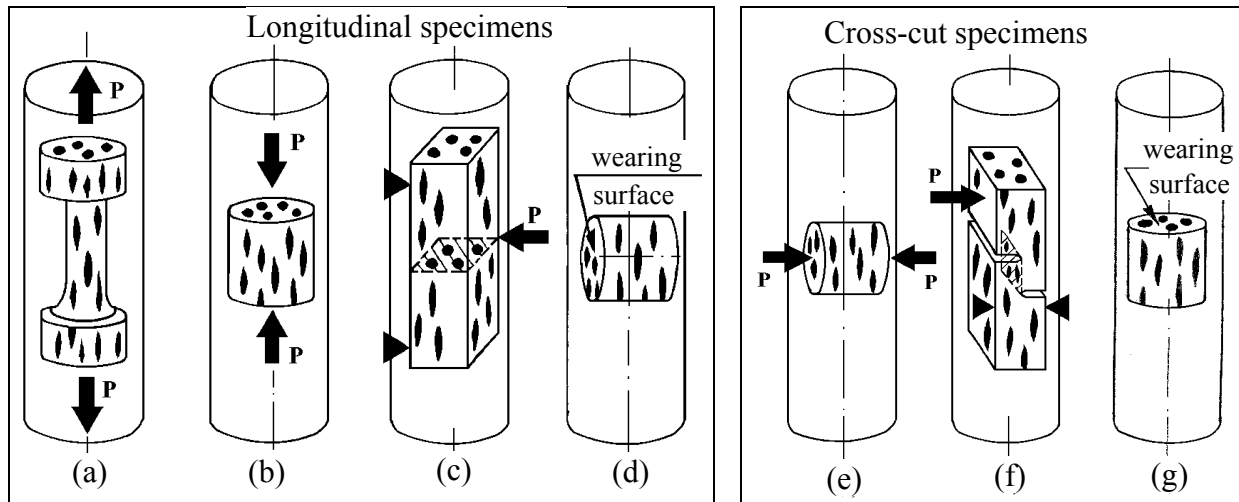


Fig. 4 Schematic of specimens cutting-out from extruded cast-iron rods for subsequent mechanical testing: longitudinal specimens for (a) tensile test, (b) compression test, (c) impact strength test and (d) wear resistance studying, and cross-cut specimens for (e) compression test, (f) impact strength test and (g) wear resistance examination

In the cross-section of a deformed rod, a substantial decrease in the inclusion size is observed; the shape of graphite inclusions changes from regular spherical to irregular spherical and then to a compact, or dense form. Starting from $\epsilon=60\%$, the occurrence of new small-sized graphite inclusions in the cross-section of unetched samples is observed, and at strain $\epsilon=80\%$ their volume fraction becomes substantially larger (Fig. 5). This is connected with the following two reasons. First, the cross-sectional plane may intersect the graphite spindles near the tips where their diameter is smaller. Second, during both heating to the deformation temperature and hot deformation itself, the nucleation of new dispersed graphite inclusions occurs. This is connected with the fact that deformation brings about an increase in the density of dislocations and dislocation nodes in the metal matrix, which can serve as nucleation sites. Besides, generation of a large amount of point defects (mainly vacancies) during deformation may bring about a short-term local increase in the diffusion coefficient of carbon atoms, which stimulates growth of the nuclei.

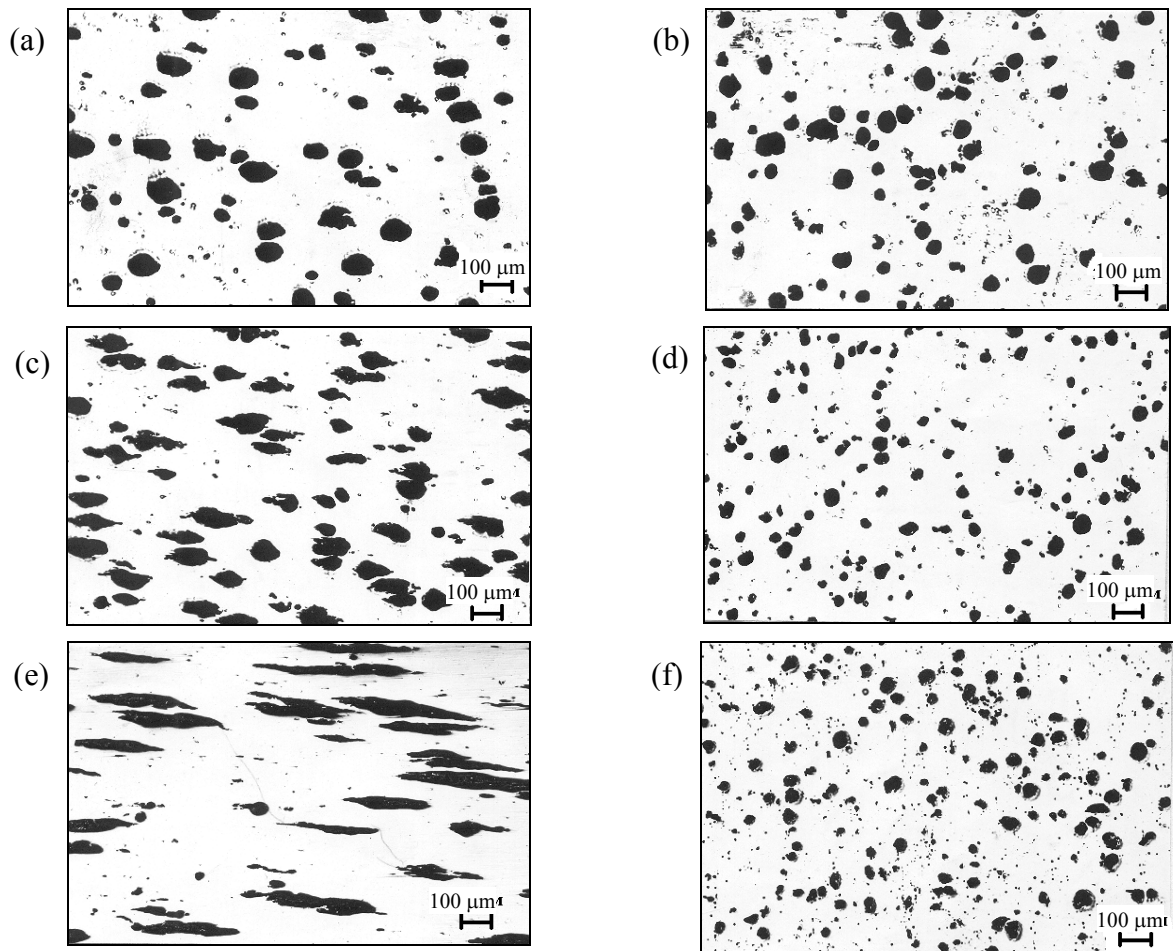


Fig. 5 Microstructure of high-strength cast iron after deformation with strain $\varepsilon=20\%$ (a and b), $\varepsilon=60\%$ (c and d) and $\varepsilon=80\%$ (e and f) for a longitudinal section (left-hand column) and cross-section (right-hand column); unetched, $\times 100$

The etched microstructures of deformed high-strength cast iron are presented in Fig. 6. As a result of deformation and subsequent air cooling, the volume fraction of pearlite has increased to about 90%.

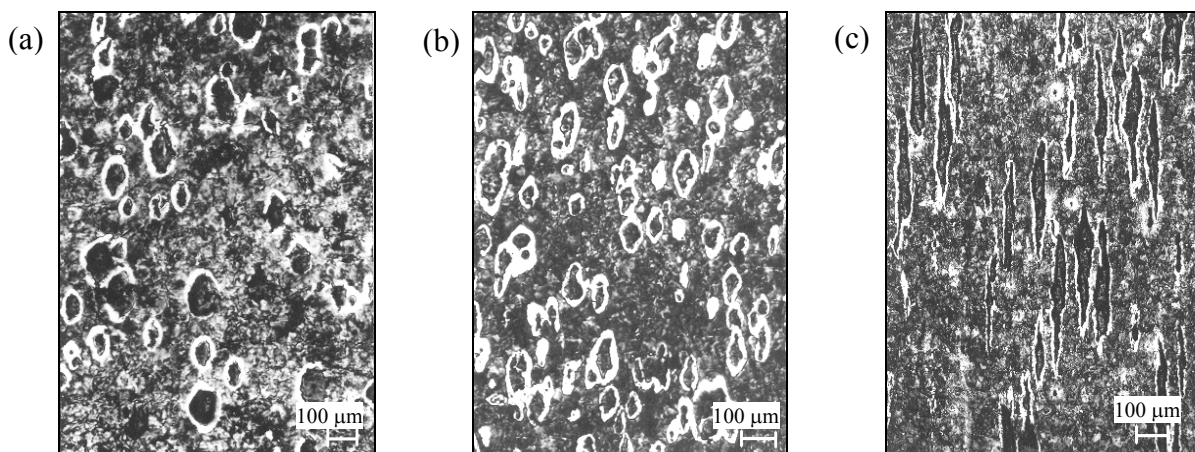


Fig. 6 Microstructure of a longitudinal section of high-strength cast iron deformed to strain $\varepsilon=20\%$ (a), $\varepsilon=40\%$ (b) and $\varepsilon=80\%$ (c); etched, $\times 100$

The transformation stages of graphite inclusions in a longitudinal section of a deformed specimen are displayed in Fig. 7. At the beginning of deformation (at small strain), an

inclusion acquires an elliptic shape with sharp ends still retaining its beam texture, which is typical of spherical graphite inclusions in high-strength cast irons (Fig. 7, a). The next stage is the formation of a diamond-shaped bulge in the central part of the inclusion and a transformation of its pointed ends into filament-like branches (Fig. 7, b). This testifies to the existence of two deformation mechanisms of graphite: shearing in the central part and plastic flow along the edges. Elongation of the filament-like branches is observed up to the strain of $\varepsilon=60\%$. In the central part, there still remains a diamond-shaped core (Fig. 7, c). Only after the strain reaches 80% (Fig. 7, d), the central diamond-like bulge disappears, the graphite inclusion stretches to acquire the shape of a spindle (Fig. 7, e) and then of a filament (Fig. 7, f).

At large strains, the formation of a large number of new small-sized graphite inclusions is observed (Fig. 7, c and d). Sometimes they contact the existing graphite particles but most often they are located separately inside the metal matrix. This can be attributed to an increase in the density of dislocations and dislocation nodes during deformation, which act as nucleation sites.

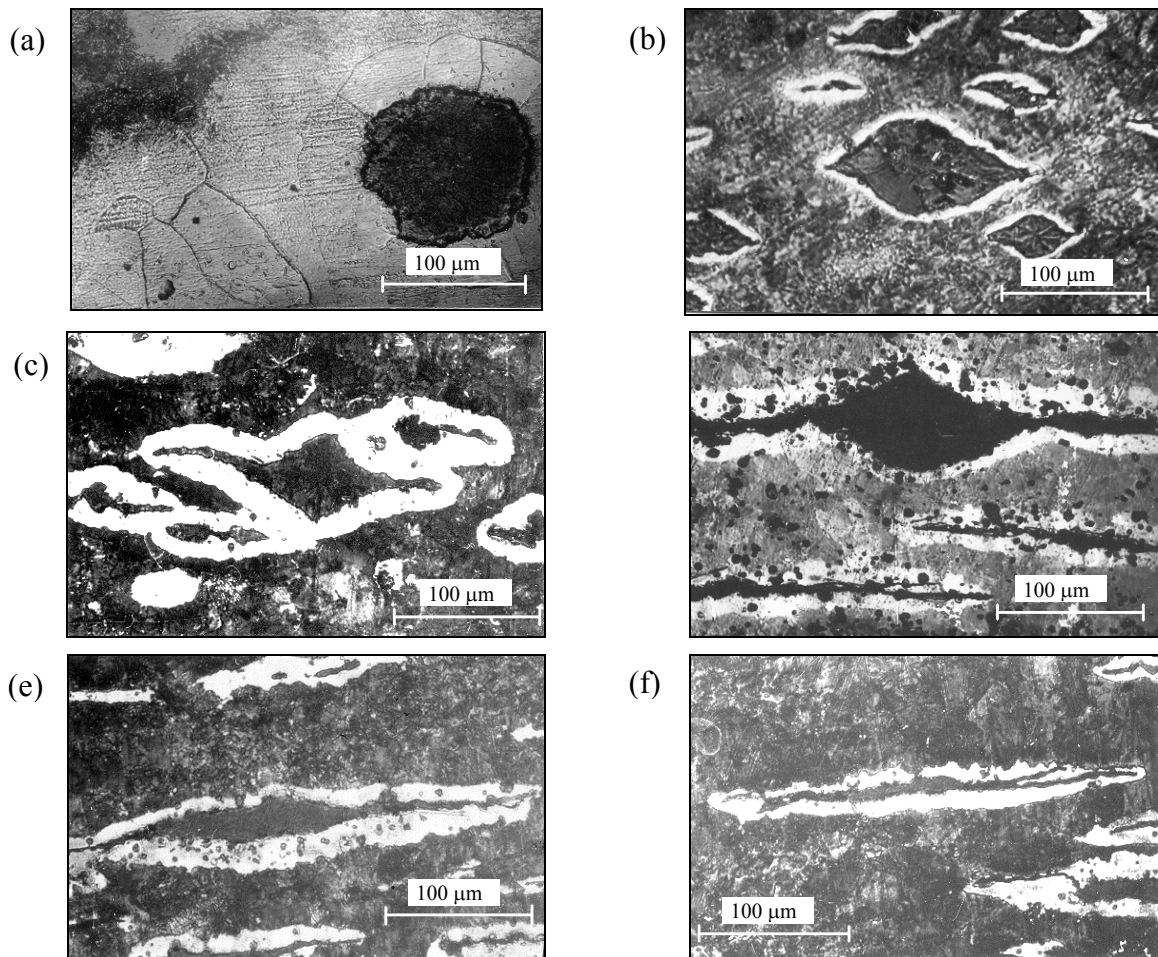


Fig. 7 Stages of shape change of an initially spherical graphite inclusion with increasing strain: (a) $\varepsilon=0\%$, (b) $\varepsilon=40\%$, (c) $\varepsilon=50\%$, (d) $\varepsilon=60\%$, (e) $\varepsilon=80\%$ and (f) $\varepsilon=90\%$; longitudinal section, etched, $\times 500$

Since cast iron is a heterogeneous material, it seems important to estimate the contribution of different structural components to strain hardening. For this purpose, specimens for tensile and compression tests have been prepared from the cast iron rods obtained by straining to $\varepsilon=20, 40, 60$ and 80% . Some of them were air cooled from the deformation temperature and had pearlitic structure. Other specimens were annealed at

950 °C for 1 h with subsequent slow cooling, which resulted in ferritic structure of the metal matrix. The samples cut out in the longitudinal direction (i.e. along the extrusion axis) were subjected to tensile tests while those cut out in the transverse direction were used for compression tests (because of their small sizes). Similar samples were prepared from the as-cast material. The results of mechanical tests are presented in Table 1.

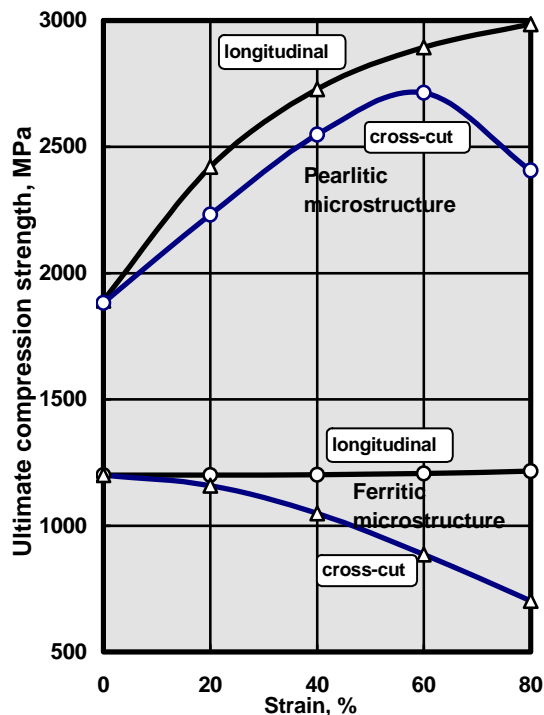
Table 1 Mechanical properties of high-strength cast iron in non-deformed (as-cast) state after different thermal processing

Properties	Heat treatment		
	as-cast	heating to deformation temperature and air cooling	ferritizing annealing
Structure of metal matrix	pearlite + ferrite	pearlite	ferrite
Ultimate tensile strength, $\sigma_B^{(t)}$, MPa	450	650	350
Elongation to failure, δ , %	5	3	8
Ultimate compression strength, $\sigma_B^{(c)}$, MPa	1500	1880	1200
Ultimate strain to crack formation during compression tests, ϵ , %	45	40	50
Hardness, HB	190	250	150

As seen from Table 1, after a ferritizing anneal the strength of cast iron decreases and the plasticity increases. Since the metal matrix in all of the specimens after annealing was composed of ferrite with a close grain size and hardness, the results of mechanical tests depended on the shape and mutual orientation of graphite inclusions.

To investigate the anisotropy of mechanical properties of differently strained cast iron, we have (i) analyzed the role of structural factors in strain hardening of cast iron and (ii) made an attempt to estimate numerically the contribution of each of these factors.

Comparative compression testing of longitudinal and cross-cut specimens of deformed cast iron with both ferritic and pearlitic structure was performed. The compression strength of longitudinal specimens with ferritic structure was found to be independent of strain, while that of cross-cut specimens was observed to decrease significantly (from 1200 to 700 MPa, i.e. by the factor of 1.7) with increasing strain from 0 to 80% (Fig. 8).



longitudinal specimens with ferritic structure was found to be independent of strain, while that of cross-cut specimens was observed to decrease significantly (from 1200 to 700 MPa, i.e. by the factor of 1.7) with increasing strain from 0 to 80% (Fig. 8).

Fig. 8 Compression strength of deformed (extruded) high-strength cast iron versus strain during extrusion.

For pearlitic structure of cast iron, longitudinal specimens exhibit an increase of compression strength by the factor of 1.6 with raising strain, and the former reaches $\sigma_B^{(c)}=3000$ MPa at $\epsilon=80\%$. For cross-cut specimens, a maximum in the dependence of $\sigma_B^{(c)}$ on ϵ is observed at $\epsilon\approx 60\%$ (Fig. 8). A decrease in compression strength at $\epsilon>60\%$ can be ascribed to unfavorable arrangement of graphite filaments, along which the fracture occurs.

Therefore, the compression strength of deformed cast iron in the direction along the axis of deformation (extrusion) is virtually independent of the aspect ratio of elongated graphite inclusions. A buildup in strength of longitudinal samples can be ascribed to an increase in the volume fraction and a decrease in the interlamellar spacing of pearlite.

A compressive stress directed across the elongated graphite inclusions has a negative effect on strength and hence service properties of the material.

The overall strain hardening of cast iron, which is observed in specimens with pearlitic structure (Fig. 8), can be ascribed to a synergetic effect of several structural factors such as (i) shape of graphite inclusions, (ii) volume fraction, morphology and dispersity of pearlite, (iii) increase in the density of cast iron due to healing of some casting defects, e.g., gas cavities, etc. Some of these factors may have an opposite effect on strength. For example, elongation of graphite inclusions and deviation of their shape from a spherical one decreases strength, while increasing the fraction of pearlite raises the latter. Decreasing the size of pearlite grains and lamellae thickness within these grains contributes to an increase in strength.

The data presented in Fig. 8 can be used for estimating numerically the role of metal matrix in strain hardening of deformed cast iron and the effect of the shape of graphite inclusions on its weakening. As a first approximation, assuming a linear dependence of the compression strength of deformed cast iron, $\sigma_B^{(d)}$, on basic structural factors, we can write:

$$\sigma_B^{(d)} = \sigma_B^{(c)} - K_1\sigma_B^{(c)} + K_2\sigma_B^{(c)} + K_3\sigma_B^{(c)}, \quad (1)$$

where $\sigma_B^{(c)}$ is the compression strength of in the as-cast state (in MPa), K_1 is a numerical factor describing a decrease in strength because of elongation of graphite inclusions (for globular graphite $K_1=1$), K_2 is a strengthening factor associated with an increase of the volume fraction of pearlite, and K_3 is a coefficient accounting for strengthening due to changes in the morphology and dispersity of pearlite, an increase in the cast iron density during extrusion, and other factors.

Using the data presented in Table 1 for non-deformed cast iron and the results of compression tests for deformed cast iron shown in Fig. 8, the values of numerical factors entering Eq. (1) were estimated as follows. Comparing the properties of cast iron with ferretic structure, i.e. after ferritizing annealing ($\sigma_B^{(c)}=1200$ MPa in Table 1), with the strength of cross-cut samples of a deformed material at $\varepsilon=80\%$ ($\sigma_B^{(d)}\approx 700$ MPa as seen from Fig. 8), we obtain $K_1=0.42$.

For estimating parameter K_2 , the compression strength of a non-deformed cast iron in the as-cast state has been compared with that for the same material after normalizing heat treatment at a temperature corresponding to the extrusion temperature (see Table 1). This is because the volume fraction of pearlite after normalizing and after deformation were close, about 90%. Using the data listed in Table 1, we obtain $K_2=0.32$.

Using Eq. (1) we can estimate the remaining parameter K_3 that characterizes the effect of the pearlite morphology and dispersity on compression strength of deformed cast iron. As seen from Fig. 8, at $\varepsilon=80\%$ for cross-cut samples $\sigma_B^{(d)}=2400$ MPa. Using the above-mentioned data, we have $K_3=0.38$.

The relative contribution of structural factors expressed by coefficients K_1 , K_2 and K_3 to the overall compressive strength is schematically shown in Fig. 9.

In regard to such factors as the volume fraction of pearlite (K_2) and shape distortion of graphite inclusions (K_1), with raising strain from 0 to 40-60% the compression strength is supposed to increase. This is connected with the fact that the fraction of pearlite increases to 90% while the shape of graphite particles still insignificantly deviates from a spherical one. At $\varepsilon\geq 60\%$, thin filament-like branches, or whiskers appear at the ends of graphite inclusions. This exerts a negative influence on strength, which cannot be compensated by an increase in

the fraction of pearlite of nor by dispersity of the latter. As a result, increasing strain from 60% to 80% results in a decrease in the compression strength, which, however, still substantially exceeds a value typical of the as-cast state. Finally, at high strains the mechanical properties decrease significantly. This can be ascribed to the fact that the content of pearlite remains almost constant while the shape of graphite inclusions continues changing thus exerting a negative effect on strength.

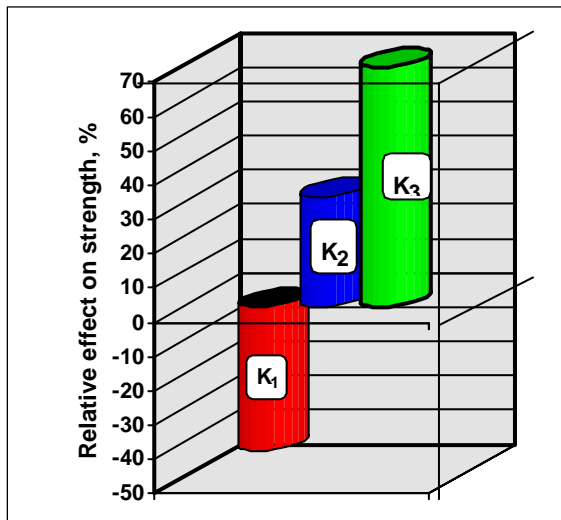


Fig. 9 Relative effect of structural factors on the mechanical properties on a deformed high-strength cast iron: elongation of graphite inclusions (K_1), volume fraction of pearlite (K_2) and a change in the morphology and dispersity of pearlite (K_3)

Since the content of pearlite reaches a high and almost constant value, about 90%, at a relatively small strain ($\epsilon \geq 20\%$), the overall strength is a result of competition between a permanent positive effect of pearlitization and increasing negative effect of the changing shape of graphite inclusions. Thus, the maximal strength is supposed to correspond to $\epsilon = 40-60\%$, which agrees with experiment (see Fig. 8).

CONCLUSIONS

1. Hot plastic deformation has a profound effect on the structure of high-strength cast iron, which refers to both graphite inclusions and metal matrix. Besides, deformation permits healing some casting defects, such as small gas cavities, which cannot be eliminated by heat treatment.

2. Extrusion brings about a pronounced texture. The shape of graphite inclusions changes with strain; the most significant shape distortion occurs at $\epsilon \geq 80\%$ in the direction parallel to the axis of extrusion and, in a much smaller degree, in the transverse direction.

3. Recrystallization that takes place during and especially after hot deformation results in the formation of a large number of small (5-8 μm) grains whose size is 3 times lower than that of initial grains. Microhardness measurements have revealed that the uniformity of the metal matrix, i.e. a difference between maximal and minimal values of microhardness, has improved by the factor of 3.5. Also, plastic deformation was observed to change the microstructure of pearlite: the lamellas become curved, lamellae spacing (i.e. dispersity) decreases from 0.7-0.9 μm to 0.3 μm .

4. Comparative mechanical testing have revealed an increase in both strength and plasticity by the factor of 1.6 after deformation and air cooling (see Fig. 8).

5. The mechanical properties of deformed cast iron were found to strongly depend on strain, direction of specimens cutting out (longitudinal or transverse) and type of metal matrix (ferritic or pearlitic). Relative changes in properties with increasing strain from 0 to 80% are presented in Table 2. Longitudinal samples (with respect to the extrusion axis) exhibit an improvement of the whole set of mechanical properties, while the cross-cut ones demonstrate a decrease in properties.

6. A transition from ferritic to pearlitic structure of the metal matrix in a deformed cast iron brings about a substantial improvement of mechanical properties in both longitudinal and transverse direction. Samples deformed at $\epsilon = 80\%$ demonstrate an increase in mechanical properties by the factor of 1.5-1.9, which raises a deformed cast iron as a structural material to

a level competitive with an alloy steel. It should be emphasized that at $\varepsilon=80\%$ the properties of cast iron even in the most unfavorable (transverse) direction exceed those of typical of the as-cast state.

Table 2 Relative changes in the mechanical properties of a deformed high-strength cast iron with increasing ε from 0 to 80%

Structure	Ferritic		Pearlitic	
	Longitudinal	Cross-cut	Longitudinal	Cross-cut
Ultimate tensile strength	increase by the factor of 1.2	decrease by the factor of 1.7	increase by the factor of 1.5-1.7	increase by the factor of 1.4
Elongation to failure	increase by the factor of 1.2	-	increase by the factor of 1.7-1.9	-
Ultimate compressive strain to crack formation	increase by the factor of 1.1	decrease by the factor of 1.6	increase by the factor of 1.5	increase by the factor of 1.1

7. The overall strain hardening of deformed cast iron observed in longitudinal specimens is due to synergetic action and competition of several structural factors: shape of graphite inclusions (factor K_1), volume fraction (factor K_2) and dispersity (factor K_3) of pearlite. Deviation of the graphite shape from spherical decreases strength, while refinement of the austenite grains and decreasing the lamellae spacing of pearlite bring about an increase in strength. The numerical values of the above factors are estimated numerically: e.g., for cross-cut specimens of high-strength cast iron deformed to strain 80%, are the following: $K_1=0.42$, $K_2=0.32$, $K_3=0.7$.

References

- [1] DUDETSKAYA, L.,R. and POKROVSKIY, A.,I. *A review of research on deformed cast irons. Vesti NAS Belarus, ser. Phys.-Techn. Nauk*, 2000, No.2, p.28-36 (in Russian).
- [2] ZHUKOV, A., A., SILMAN, G., I. and FROLTISOV, M., S. Deformed cast irons. In *Wear-resistant Casts from Alloyed White Cast Iron*. Moscow, Mashinostroenie, 1984, p.58-59 (in Russian).
- [3] LYAKISHEV, N., P. and SHCHERBEDINSKIY, G.,V. Hot plastic deformation of high-strength cast iron. In *Proceedings of 5th Congress of Metal Scientists of Russia*. Krasnodar, 2001, p. 249-251 (in Russian).
- [4] KOSNIKOV, G., A., MOROZOVA, L., M. and BEKH., N., I. Effect of hot plastic deformation on the structure and properties of cast iron with nodular graphite. *Liteynoe Proizvodstvo*, 1998, No.11, p.30-31 (in Russian).
- [5] DUDETSKAYA, L., R. and POKROVSKIY, A., I. Study of strength and plasticity of cast irons at high temperatures. In *Vesti NAS Belarus, ser. Phys.-Techn. Nauk*, 2000, No.42, p. 51-55 (in Russian).
- [6] Gvetadz, R.,G. *Development and Optimization of Deformed High-strength Cast Irons*. D.Sc. dissertation, Kiev, 1990 (in Russian).
- [7] DUDETSKAYA, L.,R., POKROVSKIY, A.,I., GAUHSSTEIN, I.,S., DEMIN, M.,I., and GURCHENKO, P., S. Deformation as a strengthening method for iron castings. In *Avtomobil'naya Promyshlennost'*, 2001, No.7, p. 30-33 (in Russian).
- [8] DUDETSKAYA, L., R. and POKROVSKIY, A.,I. Industrial testing of production technology of critical automotive parts from a deformed cast iron. In *Vesti NAS Belarus, ser. Phys.-Techn. Nauk*, 2003, No.2, p.51-57 (in Russian).